Pectin and Mucin Enhance the Bioadhesion of Drug Loaded Nanofibrillated Cellulose Films

*Patrick Laurén[1], *Heli Paukkonen[1], Tiina Lipiäinen[2], Yujiao Dong[3], Timo Oksanen[1], Heikki Räikkönen[2], Henrik Ehlers[2], Päivi Laaksonen[3], Marjo Yliperttula[1,4], Timo Laaksonen[1,5]

[1] Division of Pharmaceutical Biosciences, Faculty of Pharmacy, University of Helsinki, Helsinki, Finland
[2] Division of Pharmaceutical Chemistry and Technology, Faculty of Pharmacy, University of Helsinki, Helsinki, Finland
[3] Department of Bioproducts and Biotechnology, Aalto University, Espoo, Finland
[4] Department of Pharmaceutical and Pharmacological Sciences, University of Padova, Padova, Italy
[5] Laboratory of Chemistry and Bioengineering, Tampere University of Technology, Tampere, Finland

*These authors contributed equally

Abstract

Purpose

Bioadhesion is an important property of biological membranes, that can be utilized in pharmaceutical and biomedical applications. In this study, we have fabricated mucoadhesive drug releasing films with bio-based, non-toxic and biodegradable polymers that do not require chemical modifications.

Methods

Nanofibrillar cellulose and anionic type nanofibrillar cellulose were used as film forming materials with known mucoadhesive components mucin, pectin and chitosan as functional bioadhesion enhancers. Different polymer combinations were investigated to study the adhesiveness, solid state characteristics, film morphology, swelling, mechanical properties, drug release with the model compound metronidazole and *in vitro* cytotoxicity using TR146 cells to model buccal epithelium.

Results

SEM revealed lamellar structures within the films, which had a thickness ranging 40-240 µm depending on the film polymer composition. All bioadhesive components were non-toxic and showed high adhesiveness. Rapid drug release was observed, as 60-80% of the total amount of metronidazole was released in 30 minutes depending on the film formulation.

Conclusions

The liquid molding used was a straightforward and simple method to produce drug releasing highly mucoadhesive films, which could be utilized in treating local oral diseases, such as periodontitis. All materials used were natural biodegradable polymers from renewable sources, which are generally regarded as safe.

Keywords: Drug release; Nanofibrillar cellulose; Bioadhesion; Mucoadhesion; TR146

Abbreviations: NFC, nanofibrillar cellulose; ANFC, anionic type nanofibrillar cellulose; MZ, metronidazole

1. Introduction

Bioadhesive pharmaceutical formulations are typically designed to enhance drug bioavailability by extending the residence time of drug compounds and localizing the effect at the target site. Concurrently, they also contribute to local drug delivery formulation design (e.g. buccal or topical drug delivery), which improves bioavailability by avoiding metabolic pathways, such as first pass metabolism (1,2). Furthermore, local drug delivery systems are effective at treating site specific diseases, while avoiding drug exposure on unwanted sites. Smaller doses are required and therefore systemic exposure is often limited, which leads to reduced systemic adverse effects, as demonstrated with epothilone B encapsulated bioadhesive nanoparticles in peritoneal cancer treatment (3). Additionally, protein and peptide drugs are often unable to cross biological barriers due to the heavy enzymatic activity present in the GI-tract and liver (4). Therefore, inherently unstable drug compounds can be formulated and administered with the use of local drug delivery systems. Bioadhesion is an important property of various biological barriers, such as the oral mucosa, which can be utilized as an adhesive platform for synthetic and natural polymers. Due to the benefits of site specific treatment, new bioadhesive systems are investigated to improve both local and systemic delivery (5-7).

Nanofibrillar cellulose (NFC) has been investigated as a renewable bio-based polymer for various biomedical and pharmaceutical applications (8,9). NFC has been generally regarded as a safe, non-toxic and biodegradable material (10,11). Additionally, NFC has great modification capabilities, and structural properties that resemble collagen fibers, which provides NFC with inherent soft tissue like properties (12,13). Fiber surface modifications (e.g. TEMPO (2,2,6,6-Tetramethylpiperidin-1-yl)oxyl oxidation) enables the use of anionic type NFC's (ANFC) (14,15). ANFC fiber network contains negatively charged carboxyl groups to varying degrees on individual fiber surfaces. In the pharmaceutical field, NFC has been investigated as a controlled drug releasing film, where it was reported as an excellent film forming material (16). Additionally, NFC can affect drug release profiles in a controlled manner (17). NFC can be utilized as a reinforcing material with other polymers with or without further chemical modifications (18). For example, the addition of NFC has been shown to improve structural and adhesion properties of free-standing starch/pectin films (19). In the biomedical field NFC has been investigated as a 3D cell culture matrix (13), surgical suture coatings (20) and in other various biomedical applications (21); however, due to the biomedical device challenges regarding biodegradation in the human body, ease of access locations are preferable to enable physiological self-cleansing mechanisms (e.g. oral mucosa or the GI-tract).

The oral mucosa is fully covered with a visco-elastic layer, mucus, which is primarily constituted of mucins (22). Mucins are high molecular weight glycoproteins with a tendency to accumulate at

interfaces (23). Adsorption of mucin results in thick and well hydrated layers. Mucins have diverse roles, such as lubricants or defensive components in the mucus layer protecting against pathogens (24), but also functions as a biochemical filter that can bind nutrients and a wide variety of different compounds (25). These high binding capabilities of mucins can be exploited in pharmaceutical and biomedical sciences to design muco-/bioadhesive applications.

In this study, we have focused on renewable, inexpensive, natural biopolymers with combinations of two types of film forming materials (NFC and ANFC) and three different mucoadhesive components mucin, pectin and chitosan. We have fabricated bioadhesive films with a liquid molding method that does not require chemical modifications, therefore reducing processing steps and avoiding potentially toxic residues resulting from any chemical treatment. Mucin, pectin and chitosan are all-natural polymers with mucoadhesive properties (26-28). Mucoadhesive systems require sufficient swelling and wetting capabilities, hydrogen-bonding functional groups and polymer network entanglement (22). Mucins are highly glycosylated (up to 80%) and have a negative net charge at neutral pH (26). Mucins can form gels depending on the concentration and pH by entanglement and hydrogen bonding (23), however, the structural properties can be improved with the addition of another hydrogel-forming material, such as alginate (29). Mucins tend to aggregate and interact with each other via self-assembly due to their block co-polymeric structure (30). Therefore, mucin itself can act as an excellent adhesive component in mucoadhesive formulations. Pectin is a polydisperse polysaccharide, which primarily consists of D-galacturonic acid. Pectins are able to form gels depending on the conditions, molecular size and degree of esterification (DE). Gel strength and rate of gelation increases with high DE pectins at a constant pH (31). Gelation occurs due to hydrogen bonding, presence of divalent cations or hydrophobic interactions. High DE pectins have also shown to be highly mucoadhesive, despite having a low amount hydrogen bonding forming groups; therefore, mucoadhesion is likely caused by entanglement mechanisms (27). Chitosan is a cationic linear copolymer of (1-4)-2-amino-2-deoxy-b-d-glucan (GlcN) and (1-4)-2-acetamido-2-deoxy-b-d-glucan (GlcNAc). Chitosan has been widely used in drug delivery applications; additionally, the properties of various chitosan salts have been investigated in controlled drug delivery (32). Chitosan is characterized as highly viscous polymer, in addition to having film forming properties and bioadhesivity through electrostatic interactions (28,33). However, due to strong intermolecular hydrogen bonding, chitosan is insoluble in water at neutral pH. Therefore, it is often convenient to use chitosan in its salt form such as chitosan lactate.

The polymer compositions for mucoadhesive films were first evaluated in terms of peak force measurements with texture analysis to evaluate mucoadhesiveness, tensile strength for mechanical

properties and swelling/hydration studies without the study compound metronidazole (MZ), an antibacterial compound used to treat periodontal diseases. NFC/ANFC-mucin and NFC/ANFC-pectin films in 2:1 mass ratio (wt/wt) were selected for encapsulation of MZ. Solid state characterization with DSC, Raman and FTIR as well as imaging of morphology with SEM was then performed for selected films. Drug release studies were done with the study compound MZ to evaluate the drug release profiles from mucoadhesive films. Additionally, cytotoxicity assays were performed with human squamous carcinoma, TR146, cells to model in vitro buccal toxicity. The liquid molding preparation method used in this study was observed to be a simple and straightforward way to make mucoadhesive films. The used method could be easily scaled up with paper industry equipment that could produce large amounts of drug releasing mucoadhesive and biodegradable paper. Further, we observed that the mucoadhesive properties of NFC and ANFC could be enhanced with the incorporation of mucoadhesive components. This indicates that the mucoadhesive NFC and ANFC film formulations have potential as local drug delivery systems for site specific medication of oral diseases.

2. Materials and methods

2.1. Materials

1.5% NFC hydrogel (processed from birch pulp, UPM-Kymmene Corporation, Finland) and 2.7 % ANFC hydrogel (UPM-Kymmene Corporation, Finland) with carboxyl groups at 1.03 mmol/g of fibers were used as film forming polymers. Chitosan oligosaccharide lactate (Sigma-Aldrich, USA), mucin from bovine submaxillary gland (EMD Millipore, USA) and pectin from apple (Sigma-Aldrich, China) were used as mucoadhesive polymers in NFC and ANFC films. Microcrystalline cellulose (MCC, Avicel PH200, FMC BioPolymer, Ireland) and mucin from porcine stomach (Type-II) (Sigma-Adrich, USA) were used for the preparation of 600 mg mucin/MCC discs in 4:1 mass ratio (wt/wt) respectively. Mucin from bovine submaxillary glands (Type-I) was prepared as a 1 % solution (Sigma-Aldrich, USA) for the hydration of mucin discs prior to adhesion testing with TA.XT plus. Metronidazole (Sigma-Aldrich, China) was used as a model drug compound in mucoadhesive film formulations. Analytical grades sodium phosphate dibasic (Sigma-Aldrich, Germany) and sodium phosphate monobasic (Sigma-Aldrich, Germany) were used in the preparation of 50 mM pH 6.8 phosphate buffer. Acetonitrile (Sigma-Aldrich, Germany) was of analytical grade.

2.2. Preparation of mucoadhesive films

1% NFC or ANFC hydrogels diluted from stock concentrations 1.5% and 2.7% for NFC and ANFC respectively were thoroughly mixed with the mucoadhesive polymers (pectin, mucin or chitosan) in 10:1, 2:1 and 1:1 NFC:polymer mass ratios to the dry fiber content in NFC/ANFC. Films for mucoadhesive strength measurements were prepared by drying 4 g of the hydrogel formulation in plastic Petri dishes (Nunclon™ Delta, Thermo Scientific) with a diameter of 4 cm for 18 h at 45 °C in an oven. Films for swelling, tensile strength, solid state characterization, drug release and toxicity studies were prepared from 9.0 g of the hydrogel formulation placed in a 3D printed (Ultimaker 2+ 3D printer, Netherlands) round PLA mold with a diameter of 4 cm on top of a flat Teflon surface and oven dried for 18 h at 45 °C. For tensile strength measurements, the films were prepared without MZ as described above (Table I). In contrast, films containing MZ were prepared for the swelling study, drug release studies, SEM imaging, solid state characterization and toxicity studies. Films without MZ had NFC or ANFC with either pectin or mucin in 2:1 mass ratios. Drug containing films included MZ, whose amount was set to 10% of cellulose and polymer dry mass. The hydrogel formulations were prepared in 20 ml glass vials and all components were mixed thoroughly prior to film preparation. NFC, ANFC and mucin containing films did not shrink during oven drying and the film diameter remained at 4 cm, whereas for pectin containing films, the film diameter was reduced to 3.5 cm after drying. The films were stored at 25 °C inside a silica desiccator until used.

Table I. Solid content of NFC, ANFC, mucin, pectin and MZ in film formulations prepared from 9 g of hydrogel.

Formulation	NFC (mg)	ANFC (mg)	Mucin (mg)	Pectin (mg)	MZ (mg)
NFC	90				
ANFC		90			
NFC-Mucin	90		45		
ANFC-Mucin		90	45		
NFC-Pectin	90			45	
ANFC-Pectin		90		45	
NFC-Mucin-MZ	90		45		13.5
ANFC-Mucin-MZ		90	45		13.5
NFC-Pectin-MZ	90			45	13.5
ANFC-Pectin-MZ		90		45	13.5

2.3. Evaluation of the mucoadhesive strength of drug free films

Mucoadhesive strength of the NFC/ANFC films combined with pectin/mucin/chitosan was evaluated with a texture analyzer TA.XT plus (Stable Microsystems Ltd, UK, equipped with a 5 kg load cell) in texture profile analysis (TPA) mode. 13 mm diameter mucin-MCC (4:1 mass ratio) tablets (600 mg) were prepared in a Carver press by direct compression with a compression force of 3000 kg for 30 seconds. A double sided adhesive tape was used to attach the tablet horizontally into the lower end of a 10 mm diameter TA.XT plus probe. As the tablets were used to simulate mucosal membrane in the experiment the whole tablet surface was wetted with 150 µl of 1 % mucin solution for 20s after which the excess solution was carefully removed with a tissue paper by gentle blotting. Samples of each film type were placed under the analytical probe in flat Petri dishes and the probe was lowered until the mucin disc was in contact with the surface of the sample. The following parameters were used in the measurement: 0.50 mm/s pre-test speed, 0.30 mm/s test speed, 0.3 mm/s post-test speed, 100 g applied force, 4 mm return distance, 15 s contact time and 3 g trigger force. Results were analyzed with Exponent software (Stable Microsystems Ltd., UK) and the peak adhesion force (N) required to detach the mucin tablet from the surface of the film was used as a measure of mucoadhesive strength. All measurements were performed at least in triplicate.

2.4. Tensile strength test of drug free films

Tensile tests were performed in a controlled humidity chamber with the tensile tester (Kammrath & Weiss GmbH, Germany) in Tensile/Compression Module 5 kN with a 100 N load cell. The films were equilibrated at 50 % relative humidity and stored at 20 ˚C overnight before the tensile test, to minimize the contribution of the varying ambient humidity in the tensile results. Sample sizes were 20 x 2 mm, length and width respectively. Film thickness was measured by the displacement sensor (LGF-0110L-B, Mitutoyo, Japan) with a digital reader (EH-10P, Mitutoyo, Japan). The samples were displaced on a measuring table with a support for displacement sensor (215−514 comparator stand, Mitutoyo, Japan). The measurements were performed at least 3 times for each sample. The Young's modulus (YM), tensile strength, elongation and toughness were calculated from the average of strain-stress curves that were obtained by dividing the tensile load curve with the cross-sectional area of the respective sample. The Young's modulus was taken as the slope of the elastic region of the curve, whereas the tensile strength and elongation were taken as the values at the point of fracture. The tensile toughness was estimated as the work-of-fracture obtained by integrating the area under the stress curve.

2.5. Swelling studies of drug free film formulations

Films that contained NFC or ANFC in combination with pectin or mucin (in 2:1 mass ratio) were cut into approximately 1 cm^2 surface area pieces and immersed into 50 mM pH 6.8 phosphate buffer for 15 s or 5 h at 25 °C. The film weight was measured prior to and after the hydration period in the buffer. After immersion, the excess buffer on the surface of films was wiped off before weighing. After this the films were dried for 20 h at 45 °C, cooled for 1 h and weighed again. The increase in weight of the patches (n = 3) was determined for both the 15 s and 5 h time point samples. The hydration percentage was calculated with the following equation:

$$\textbf{Hydration \%} = (X_t - X_0) / X_0 \times 100 \quad (1)$$

where X_t is the weight of the swollen sample and X_0 is the original weight of the sample. The mass of the original sample was compared to the corresponding weight after the swelling test and re-drying to obtain mass loss percentage as follows:

$$\textbf{Mass loss \%} = (X_0 - X_d)/X_0 \times 100 \quad (2)$$

where X_d is the weight of the re-dried sample. For formulations that were tested in the drug release studies, the swelling was evaluated after 30 min exposure to the release buffer. Here the dimensions (thickness n = 5, surface area n = 1) of the original samples were compared to values obtained after 30 min from digital camera images. Image J software (National Institutes of Health, Bethesda, USA) was used to measure the film dimensions. The original dry film thickness was obtained from SEM images (n = 10) and the surface area in dry and wetted state, as well as thickness in the wetted state were obtained from digital camera images with ImageJ software (National Institutes of Health, Bethesda, USA).

2.6. Differential scanning calorimetry (DSC)

Thermal analysis of selected films was carried out using a differential scanning calorimeter Mettler Toledo DSC 823e (Mettler Toledo, Giessen, Germany, calibrated by indium: Tm 156.6, heat of fusion 28.21 J/g). The film samples as well as pure MZ, pectin, mucin, NFC and ANFC of 1-3 mg were placed in aluminum pans with perforated lids and heated at a scanning rate of 10 °C/min between 25 and 220 °C in nitrogen atmosphere. The obtained data was analyzed with STARe software (Mettler-Toledo, Giessen, Germany), and the onset temperatures were used as melting point values.

2.7. Fourier-transform infrared spectroscopy (FTIR)

ATR-FTIR spectroscopy was carried out to characterize the films, using a Vertex 70 FTIR spectrometer (Bruker Optik GmbH, Germany) with a MIRacle^{TM} single reflection ATR crystal (Pike Technologies, Inc., USA). The analytical range in the measurements was 650 to 4000 cm^{-1} with a

spectral resolution of 4 cm^{-1}. Each spectrum was the average of 64 scans and three spectra were collected for each sample. Principle component analysis (PCA) was used to evaluate the data, and it was performed with standard normal variate (SNV) transformed and mean-centered spectra using SIMCA software (Sartorius Stedim Biotech, Sweden).

2.8. Raman spectroscopy

Raman spectroscopy analysis was performed for the films with a Raman RXN1 spectrometer, equipped with a PhAt probe head and a 20-mW laser source operating at 785 nm (Kaiser Optical systems, Inc., USA). Each spectrum consisted of an average of three scans recorded with an integration time of 1 s, apart from the NFC and ANFC control films for which ten scans with 3 s integration time were averaged. The samples were measured in triplicate. The spectra were analyzed after removal of elevated baselines using a rubberband correction method (Opus software, Bruker Optik GmbH, Germany). The spectra were normalized by SNV transformation and mean centering before analysis by PCA (SIMCA software, Sartorius Stedim Biotech, Sweden).

2.9. Scanning electron microscopy (SEM)

The morphology of the films was imaged with a scanning electron microscope Quanta FEG250 (SEM, FEI Company, USA). The films were fractured manually for analysis of the inner film structure. Micrographs of the cross-sections as well as surface structures of the films were obtained. Prior to SEM imaging the samples were fixed onto a two-sided carbon tape and sputtered with platinum for 25s with an Agar sputter device (Agar Scientific Ltd., UK).

2.10. Release of metronidazole from mucoadhesive film formulations

The release of MZ was tested with an incubator shaker Titramax 1000/Incubator 1000 (Heidolph, Germany) at 37 °C with 200 rpm. The film dosage forms were cut into squares with an area of 1 cm^2 and placed inside glass vials. The weight (n = 3) of the film pieces varied according to formulation as follows: 12.7 ± 0.1 mg (ANFC-Mucin-MZ), 16.5 ± 1.5 mg (NFC-Mucin-MZ), 23.6 ± 2.8 mg (ANFC-Pectin-MZ) and 23.4 ± 3.0 mg (NFC-Pectin-MZ). The glass vials were filled with 10 ml of 50 mM pH 6.8 phosphate buffer and the film pieces remained immersed in the release buffer throughout the release study. 0.5 ml samples were collected at predetermined time points up to 30 min and replaced with 0.5 ml of fresh buffer. Samples were filtered through 0.2 µm PTFE membranes (VWR International, USA) and diluted to 1:10 with 0.015 mM pH 2 phosphate buffer prior to UPLC analysis. The samples were analyzed with Ultra performance liquid chromatography (UPLC) instrument Acquity UPLC (Waters, USA). Sample injection volume was 10 µl and the used column

was Primesep 100 5 µm (2.1 x 50 mm) (Waters, USA) at 30°C. The mobile phase during the isocratic run consisted of 20/80 of ACN/15mM phosphate buffer pH 2 and the flow rate was 0.5 ml/min. The detection of MZ was performed at 317 nm wavelength and the retention time of MZ was 1.04 min. The linear concentration of MZ was established at 0.5 - 50 µg/ml and LOD for MZ was 0.03 µg/ml. All release studies were performed in triplicate.

2.11. Toxicity studies with TR146 human buccal epithelium model

Human squamous cell carcinoma, TR146, was purchased from Sigma-Aldrich (passage #9, 10032305, ECACC, UK). Cells were cultured in Dulbecco's Modified Eagle Medium: Nutrient Mixture F-12 (DMEM/F-12, Gibco™, Thermo Fisher, USA) supplemented with 10 % Fetal Bovine Serum (FBS, Thermo Fisher, USA) and 2mM L-glutamine (GlutaMAX™, Thermo Fisher, USA). Cells were subcultured and incubated at 37 °C, 5 % CO_2. After reaching 70-80 % confluency, the cells (at passage #12) were detached and seeded into a standard cell culture 96-well plate for cytotoxicity studies ($2x10^4$ cells/well). Bioadhesive films were prepared as described earlier. Round pieces (Ø = 5 mm, n = 4) were cut and inserted into the wells with and without cells. TR146 cells were incubated with the film pieces for 24 hours. After the incubation, the film pieces were removed and the cell proliferation reagent resazurin (alamarBlue®, Thermo Fisher, USA) was introduced into the wells according to manufactures instructions. Well plate was measured with Varioskan LUX multimode microplate reader (Thermo Fisher, USA), excitation and emission wavelengths were 565 nm and 585 nm respectively.

3. Results and discussion

3.1 Mucoadhesive strength of films

We first explored which of our test polymers would show the highest mucoadhesion strengths and in which ratio it should be mixed with NFC or ANFC. Cellulose films combined with pectin, mucin and chitosan in different mass ratios (10:1, 2:1, 1:1 wt/wt) were studied with a texture analysis technique. The technique has been widely used to evaluate the in vitro mucoadhesion of various formulations such as films, tablets and hydrogels with mucin discs or porcine buccal mucosa as binding substrates (2,27,34,35). It is known that pectin, mucin, and chitosan all have strong mucoadhesive properties (26-28), and it was expected that this technique would be suitable to determine the relative mucoadhesive strengths of these materials. Further, texture analysis measures the adhesion strength from a relatively large surface area and gives a good indication about the adhesiveness of a real drug formulation that would be based on these materials. The adhesive strength between the polymer and

the substrate after the application of an external force can be measured and is typically presented as work of adhesion (work necessary to overcome attractive forces) or peak force (maximum force required to detach the mucin disc from the formulation).

Different parameters were investigated to evaluate the strength of mucoadhesion in order to optimize the measurements. It has been shown that contact time and force have the greatest impact in mucoadhesiveness, while pre-hydration time and test speed affect to a lesser extent (27). In our study we investigated contact force (Fig. 1) and contact time (data not shown). Contact force had a great impact in the mucoadhesiveness strength. A standard keyboard key was pressed with the TA.XT plus instrument with a force of 50, 75 and 100 g (data not shown). The force of 100 g was selected for the studies, which exceeded the force required for a keystroke to register (75 g and lower did not). Higher contact forces were considered. However, in practical use the higher forces are not applicable when administering a buccal patch. Similarly, contact time for over 15 seconds would not be feasible in actual use; therefore, a contact time of 15 seconds was selected for mucoadhesive studies. After optimization, the mucoadhesiveness measurements suggest that the gentle pressure of 100 g was enough for mucoadhesion to occur and strong enough to be measured.

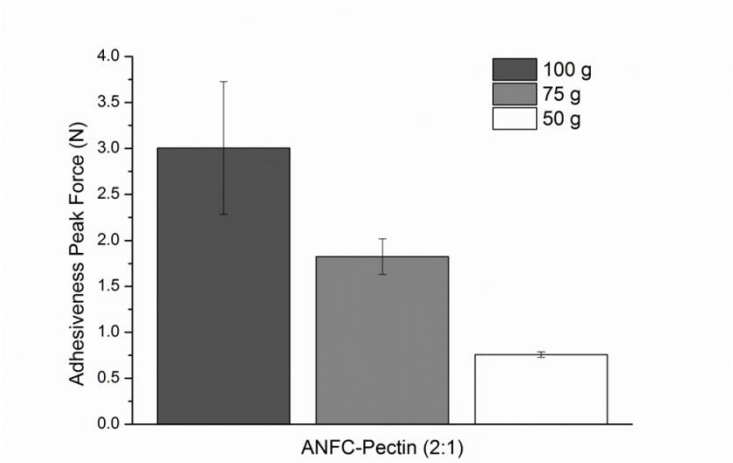

Fig. 1. The adhesiveness test of ANFC-Pectin (2:1 mass ratio) film with different contact forces 50g, 75g and 100g (n = 3 ± stdev).

Hydrated mucin discs were selected to model the mucosal layer in vitro and the adhesiveness of formulations was evaluated by comparing adhesiveness peak forces. The results are presented in Fig. 2. Parafilm was used as a negative control and a double sided adhesive tape as a positive control with peak forces of 1.1 ± 0.2 N and 3.7 ± 0.2 N respectively. Plain ANFC and NFC films had a higher adhesiveness to mucin discs that parafilm with peak forces of 1.6 ± 0.2 N and 1.6 ± 0.3 N respectively. The adhesiveness of the two-component films was increased when NFC or ANFC mass ratio to

polymer was lowered from 10:1 to 2:1. ANFC-Pectin (2:1) and NFC-Mucin films had the best adhesiveness with peak forces of 3.0 ± 0.7 N and 2.9 ± 0.2 N respectively.

For NFC containing films, mucin (2:1) was clearly the best combination in terms of adhesiveness followed by pectin and chitosan. As it is known that besides mucin, pectin can also bind to cellulose (36), it is possible that not all hydrogen bonding groups in pectin are available for the mucoadhesion process, but are used in the polymer-polymer interactions with hemicellulose, as it has been noted that birch pulp derived NFC contains even up to 23% hemicellulose residues (16). This resulted in mucin being the strongest mucoadhesive component in combination with NFC. NFC-Chitosan films could also suffer from electrostatic polymer-hemicellulose interactions, which might explain why the mucoadhesive strength was not as high as with mucin. As the groups responsible for hydrogen bonding are used in the interactions between chitosan and hemicellulose they are not available for mucoadhesion. Furthermore, chitosan is insoluble at neutral pH, and when mixed with NFC, chitosan hinders the wetting/hydration of the film surface (37), which is an important factor in mucoadhesion. In contrast to the NFC results, ANFC films with pectin (2:1) proved to have the highest adhesion followed by mucin and chitosan. This could be explained with the lack of hemicellulose in ANFC, which improved the mucoadhesion by reducing the polymer-polymer interactions that were present in NFC-Pectin. Additionally, ANFC-Chitosan film mucoadhesiveness also suffers from electrostatic interactions, as the carboxyl groups present in ANFC interact with the positively charged chitosan, and therefore all the available groups for hydrogen bonding are not available for the mucoadhesion process.

When 1:1 mass ratio was used for polymer composition, a reduction in adhesiveness was observed for all NFC films and ANFC-Pectin. Furthermore, even the formation of NFC based films suffered from an excessive amount of the mucoadhesive component. It was therefore decided that 1:1 formulation was not suitable for mucoadhesive formulations. Based on the mucoadhesive strength profiles, NFC and ANFC films combined with either pectin or mucin in 2:1 mass ratios respectively were selected for mechanical strength and swelling studies. These inherent properties of the films were evaluated prior to drug encapsulation in order to recognize how the mucoadhesive polymers influenced mechanical strength and swelling of the films when compared to plain NFC and ANFC films. Further solid state, morphology, drug release and toxicity characterization was performed with films that contained encapsulated MZ.

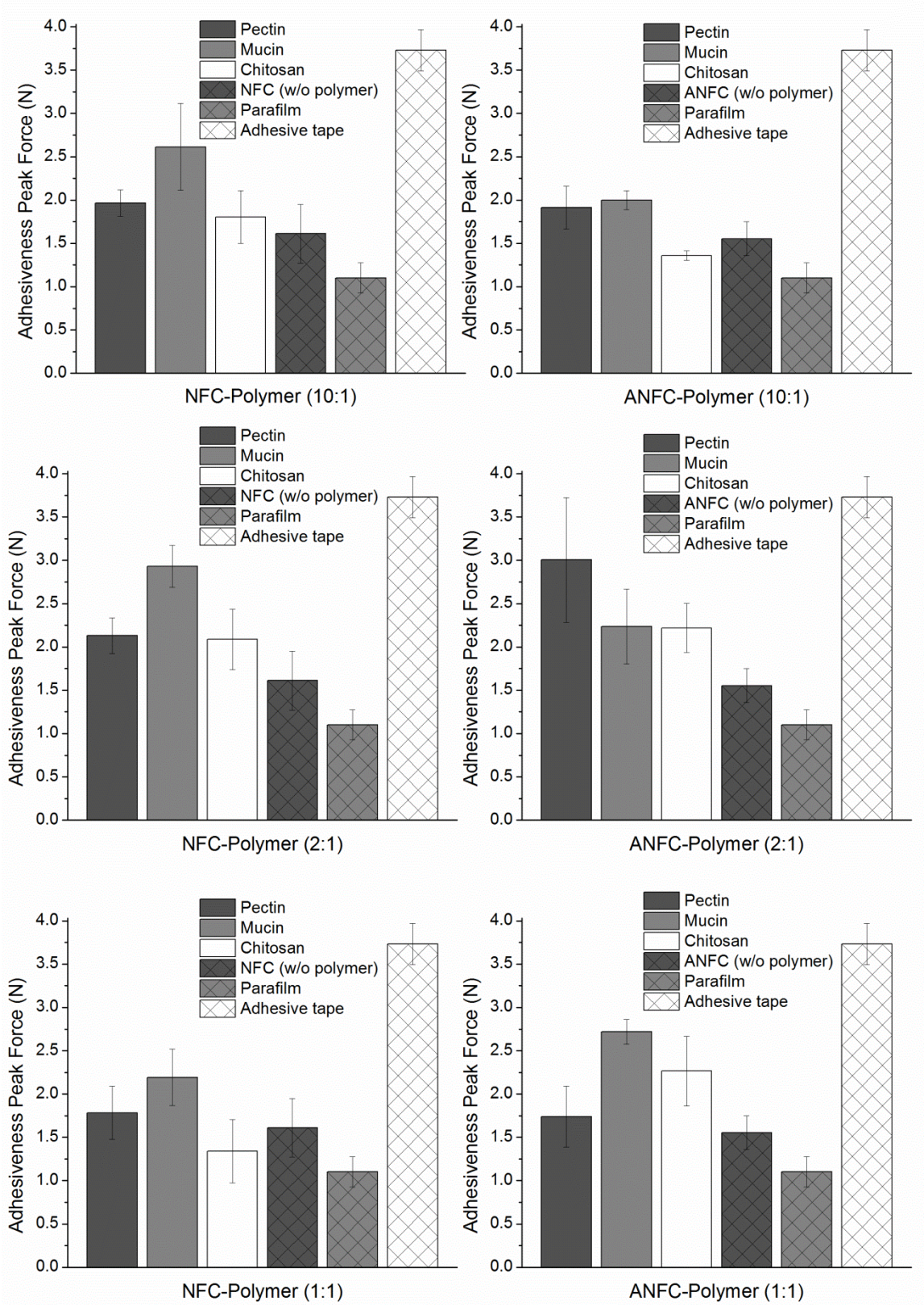

Fig. 2. Mucoadhesive strength presented as the peak force of adhesiveness for NFC and ANFC films combined with pectin, mucin and chitosan in different mass ratios (10:1, 2:1, 1:1; n = 3 ± stdev).

3.2 Tensile strength test

Mechanical properties were measured in order to evaluate and compare the tensile strength (MPa), elongation (%), Young's modulus (GPa) and toughness (MJ/m3) of films having different composition. The results of the tensile test as well as the film thicknesses are reported in Table II. Based on the measured film thickness, it appears that ANFC material formed almost 30 % denser film than NFC with the film casting method. The measured Young's modulus for NFC film at 3.6 GPa was lower than the values reported in the literature, which are typically in the 6-13 GPa range (38,39). The preparation method and film porosity affect greatly the Young's modulus values (39). The solvent casting method applied here, resulted in higher porosity and therefore in lower stiffness than samples prepared by, for instance, fiber spinning or vacuum filtration (40). ANFC film had a higher Young's modulus, 5.8 GPa, a relatively close to the reported literature value of 10 GPa (41). The higher YM is most likely due to the higher fibril density in the films compared to the NFC.

The addition of either mucin or pectin increased the film thicknesses for both cellulose grades significantly. The diameter of the pectin-containing films reduced from 4 cm into 3.5 cm during the oven drying resulting in films with 70 % and 230 % higher thicknesses compared to the NFC and ANFC films respectively. Notably, despite the lower density, all the NFC formulations with pectin or mucin had higher YM, maximal tensile strength, maximal stain and toughness resulting in films with a higher mechanical strength than the corresponding ANFC ones. The addition of either mucin or pectin into NFC films also increased the Young's modulus of the films resulting, whereas the opposite was observed for ANFC formulations as the addition of these polymers into the films reduced the Young's modulus and therefore film stiffness. The increase on the overall performance of the NFC films upon addition of the other components indicates that pectin and mucin could increase the strength of the interaction of the cellulose fibrils acting thus as cross-linkers. However, addition of pectin and mucin did not increase the toughness of the materials, but the films became more brittle, which may be a consequence of the low density. The mechanical properties of the ANFC with pectin and mucin were significantly lower than with the films consisting of ANFC only. Likely, the reason is the repulsion due to the negative charges of the components, which could prevent the cross-linking of the ANFC fibrils with the other polymers and was also the reason for the strong volume changes during film drying. The strong variation of the film densities complicates the direct comparison of the film tensile properties, but based on the data, an understanding of the structure and properties relation of the different formulations could be drawn.

Table II. Thickness, tensile strength, elongation, Young's Modulus and toughness of various formulations (n=5 ± stdev). Abbreviation YM refers to Young's Modulus.

Formulation	Film Thickness (µm)	Tensile strength (MPa)	Elongation (%)	YM (GPa)	Toughness (MJ/m^3)
NFC	95.0 ± 11.4	83.0 ± 29.0	10.3 ± 3.0	3.6 ± 1.6	6.0 ± 4.0
ANFC	68.0 ± 5.6	65.8 ± 28.2	3.9 ± 2.0	5.8 ± 1.3	2.2 ± 1.4
NFC-Mucin (2:1)	128.9 ± 29.5	82.7 ± 10.2	4.1 ± 2.1	5.9 ± 0.8	2.3 ± 1.3
ANFC-Mucin (2:1)	129.2 ± 16.5	30.0 ± 3.8	4.1 ± 1.1	2.9 ± 0.1	0.9 ± 0.4
NFC-Pectin (2:1)	161.4 ± 30.9	75.7 ± 11.7	3.9 ± 0.3	5.6 ± 1.0	2.0 ± 0.4
ANFC-Pectin (2:1)	231.0 ± 47.7	27.0 ± 4.0	2.2 ± 1.1	2.8 ± 0.7	0.4 ± 0.3

3.3 Swelling studies

At first the swelling studies were performed without the model drug compound MZ, as the release of MZ from the films would have affected the evaluation of polymer mass loss % and hydration %. Hydration % includes water uptake and swelling of the polymers as well as physical filling of the porous structure in the films. Mass loss corresponds to the loss of material during the swelling study and indicates whether the films stay intact or whether the polymers are eroded from the films. The selected films were cut into 1 cm^2 pieces (Fig. 3) and immersed into phosphate buffer for 15 s or 5 h in order to evaluate both fast wetting and hydration of films during prolonged exposure to the buffer simulating the pH of oral cavity.

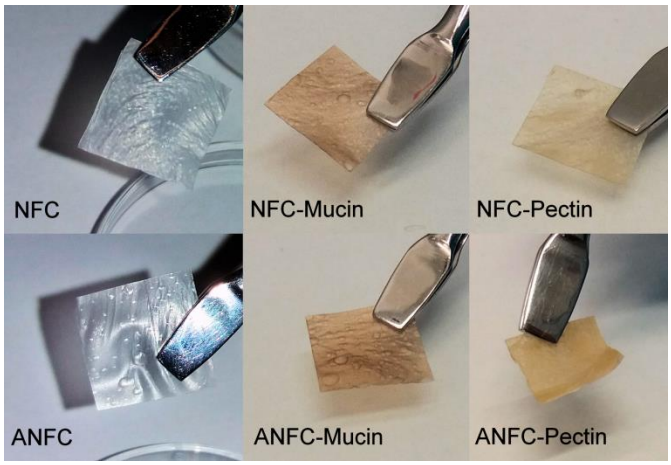

Fig. 3. Plain NFC and ANFC films and films with mucoadhesive polymers used in the swelling studies.

The hydration profiles of NFC and ANFC based films were rather similar (Table III). However, plain ANFC films were hydrated to a greater degree than NFC films with 144 % hydration at 15 s and 436.8 % hydration at 5 h. For NFC films, the corresponding values were 89.9 % and 176.1 %. NFC films are hydrophilic due to an abundance of hydroxyl groups in the molecular structure (42). However, TEMPO oxidation can be reportedly used to increase the hydrophilicity of NFC as the oxidation introduces carboxyl groups directly on ANFC surface and effectively reduces the contact

angle of water from 44° to 15° depending on the oxidation time (43). This most likely to attributes for the higher hydration % for plain ANFC based films in comparison to the NFC ones. The mass loss of plain cellulose films was quite low, indicating that the films do not degrade or erode in plain water, as was expected of these materials.

Both mucin and pectin-containing films had slower but more extensive hydration in comparison to the plain films. The hydration was lower at the 15 s time point, but higher after 5 h. In the fast 15 s hydration test the mucin containing formulations were wetted more effectively than the pectin formulations resulting in higher hydration %. However, after the 5 h test it was apparent that the pectin formulations were hydrated to a greater degree. Both mucin and pectin are very hydrophilic and can retain large amounts of water, which likely contributed to the high hydration % (44). Pectin especially is known to exhibit swelling and matrix erosion, when exposed to aqueous media, a property that has been used beneficially in controlled drug release applications (45). Here, pectin based formulations had the highest swelling % and mass loss % after 5 h exposure to the buffer ranging from 467.8 % hydration for NFC-pectin to 682.7 % for ANFC-pectin films and 21 – 32 % mass loss. As the mass loss of plain NFC and ANFC was below 5 %, the mass loss in pectin containing films is caused by pectin erosion from the lamellar film structure. Due to the considerable hydration and swelling, the NFC-pectin and ANFC-pectin films are expected to provide resistance and control to drug diffusion out of the lamellar film matrix.

Table III. Hydration of the films after 15 s or 5 h exposure to pH 6.8 phosphate buffer (n = 3 ± stdev) and mass loss after drying of the hydrated films. Mass ratio of NFC/ANFC to mucin/pectin was 2:1.

Swelling studies in pH 6.8 phosphate buffer for 15 s or 5 h						
Formulation	mg water/ mg film, 15 s	Hydration (%), 15 s	Mass loss (%) after drying	mg water/ mg film, 5 h	Hydration (%), 5 h	Mass loss (%) after drying
NFC	0.9 ± 0.1	89.9 ± 7.1	3.1 ± 0.8	1.8 ± 0.0	176.1 ± 4.3	0.6 ± 0.9
ANFC	1.7 ± 0.4	144 ± 12.1	4.6 ± 0.2	4.4 ± 0.1	436.8 ± 0.2	4.6 ± 0.2
NFC-Mucin	0.7 ± 0.3	52.3 ± 17.7	2.3 ± 0.3	4.3 ± 0.0	430.5 ± 3.8	12.2 ± 0.2
ANFC-Mucin	1.2 ± 0.1	123.5 ± 11.4	3.3 ± 1.2	5.2 ± 0.0	516.0 ± 3.4	12.5 ± 0.3
NFC-Pectin	0.7 ± 0.3	48.2 ± 9.8	4.3 ± 2.3	4.8 ± 0.0	467.8 ± 19.4	32.0 ± 1.3
ANFC-Pectin	0.5 ± 0.0	48.5 ± 0.6	4.6 ± 2.1	6.8 ± 0.0	682.7 ± 4.1	21.3 ± 0.5

3.4 Solid state characterization and morphology

The DSC thermograms revealed similar behavior for all films as the melting point of MZ was reduced from 159.8 °C, which was the melting point of pure MZ obtained in this study (Fig. 4A). The melting peaks may disappear or shift in DSC thermograms if the drug and polymer matrix are well integrated. Valo et al. have previously shown that the NFC grade and manufacturing source may affect the extent of drug interactions in freeze-dried cellulose formulations (46). Therefore, the observed differences in the melting points of MZ, may indicate interactions between the NFC/ANFC fibers and MZ. MZ had relatively small reduction in the melting point in NFC-Mucin-MZ (156.1 °C), ANFC-Mucin-MZ (157 °C) and ANFC-Pectin-MZ (155.8 °C) films. Whereas, the melting point was reduced rather significantly in NFC-Pectin-MZ (146.8 °C) films. Additionally, the DSC thermograms of individual polymers showed that there were no significant thermal changes at the range of 120-180 °C (Supporting Information; Fig. S1).

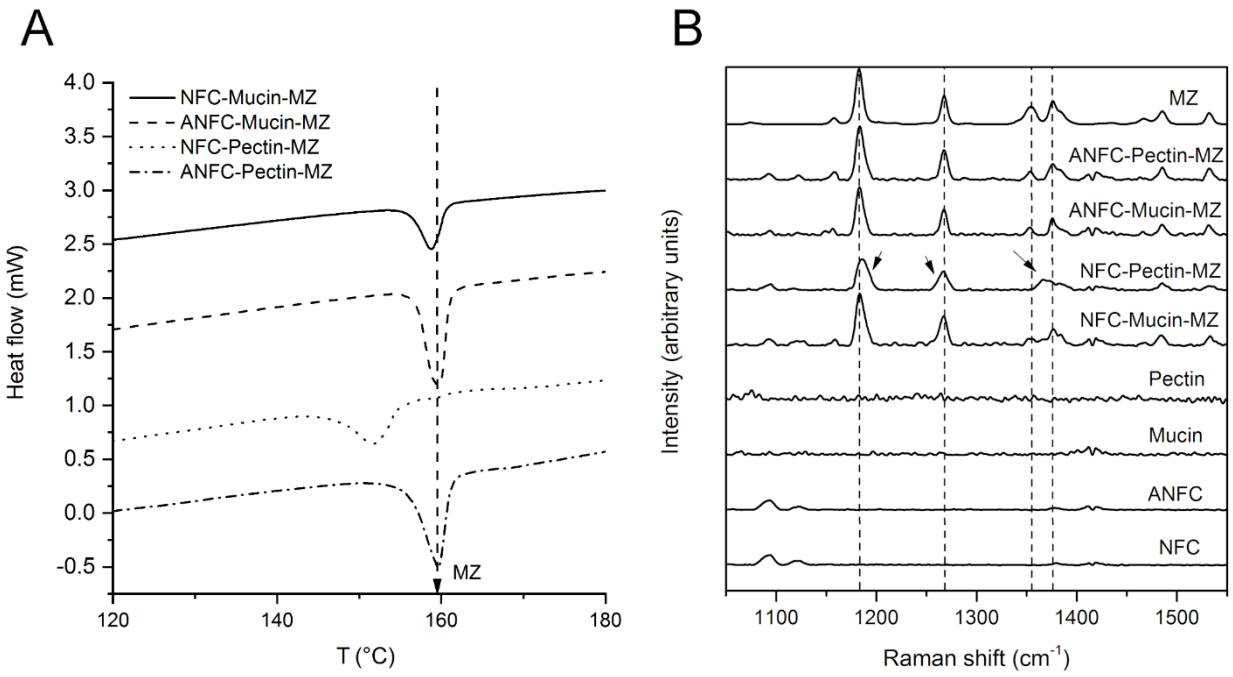

Fig. 4. DSC thermograms of films (A) and Raman spectra of single components and film formulations (B). The melting point of pure MZ at 159.8 °C is marked with a dashed line and arrow (A) and characteristic Raman peaks for MZ are marked with a dashed line (B). Broadening and shifting of MZ peaks are marked by arrows in the NFC-Pectin-MZ film.

The Raman spectra of the single components as well as film formulations are shown in Fig. 4B and characteristic bands of MZ, NFC, ANFC, pectin and mucin from literature are listed in Table S1 (Supporting Information). Raman spectroscopy revealed broadening and shifting of the MZ peaks in the NFC-Pectin-MZ film. FTIR spectra showed the presence of all components in the films

(Supporting Information; Fig. S2). Raman spectrum of pure MZ exhibits peaks at 1183 cm^{-1}, 1267 cm^{-1}, 1354 cm^{-1} and 1376 cm^{-1}. The peaks were observed for all MZ-containing film formulations. Principal component analysis (PCA) revealed that the Raman spectrum of NFC-pectin-MZ differed from all other films (Supporting Information; Fig. S3). The spectral variation between the films is due to broadening and shifting of the MZ peaks in the NFC-pectin film (marked by arrows in Fig. 4B). This variation is likely due to binding interactions between pectin side chains and NFC, and a consequent interaction with MZ, which differs from the other films (36,47). The peak widening at 1183 cm^{-1} may be indicative of intermolecular hydrogen bonding between pectin, NFC and MZ (48-52). The peak shifting of 1267 cm^{-1} to a lower wavenumber may also indicate presence of hydrogen bonding among MZ, pectin and NFC. Further, the widening of MZ at 1354 cm^{-1} and 1376 cm^{-1} may also indicate the formation of hydrogen bonds (48).

It is possible that NFC and pectin polymers may have favorable interactions for MZ encapsulation during the drying of the NFC-pectin-MZ film as all other films had only a slight decrease in the melting point of MZ. According to literature, pectin-cellulose interactions in plant cell walls may result in the intermediate binding affinity of pectin into cellulose via neutral pectin side chains or mechanical tethering between cellulose fibrils that reduces cellulose-cellulose interactions (53-55). Hemicellulose components (e.g. xyloglycan) reportedly also have binding affinity to pectin in addition to cellulose fibers and the pectin interaction with cellulose microfibrils is limited to the microfibril surface (47). The MZ in the homogenously mixed hydrogel starting material may be entrapped more effectively in the entangled polymer matrix during drying due to the binding affinity between NFC and pectin. The hemicellulose content in NFC may also attribute favorably to the possible interaction. The observation is supported by different solid state properties of NFC-Pectin-MZ films when compared to the other formulations. Interestingly, similar behavior is not observed for ANFC-Pectin-MZ films. Here the surface of ANFC fibers is coated with carboxyl groups which may be the reason for lack of binding interaction with pectin as there are fewer neutral binding sites in ANFC fiber structure and also the lack of hemicellulose content.

Cross-sectional SEM images of ANFC and NFC films revealed a lamellar structure with film thicknesses of 40.2 µm and 45.3 µm respectively (Fig. 5). The film thicknesses observed in SEM were smaller than the measurements with surface tapping method (Table II), which is due to storage of the samples in higher humidity and subsequent swelling before the tensile testing. However, ANFC films were thinner when compared to NFC films indicating that ANFC was more densely packed after drying. The addition of mucin or pectin into the ANFC films increased the film thicknesses to 97.6 µm (ANFC-Mucin-MZ) and 107.6 µm (ANFC-Pectin-MZ); however, the structure remained as

densely packed films as can be seen from the SEM images (Fig. 6). For NFC based films, the addition of mucoadhesive polymers increased the film thicknesses to a greater extent with total thicknesses of 238.8 µm (NFC-Mucin-MZ) and 228.2 µm (NFC-Pectin-MZ). The apparent porosity of NFC films observed in SEM micrographs was higher than for ANFC based films. Additionally, the NFC film lamellar structure was looser under visual inspection compared to the NFC films containing mucoadhesive polymers. Especially the NFC-Pectin-MZ films were notably denser and slightly thinner, probably due to interactions with pectin and NFC fiber network (36). Metronidazole crystals were observed in the SEM images on the surface of the film and within the lamellar structure.

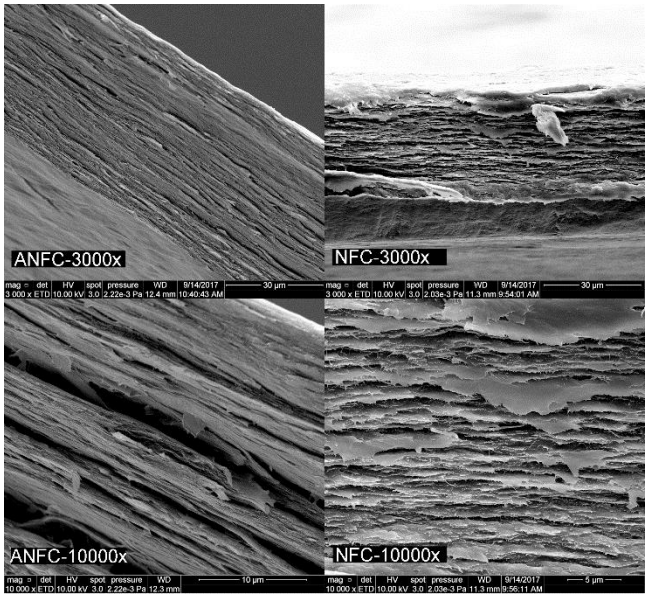

Fig. 5. SEM micrographs of ANFC and NFC films at 3000 and 10000 times magnification. The scale bar is 30 µm (top row) and either 10µm or 5µm (left to right on bottom row).

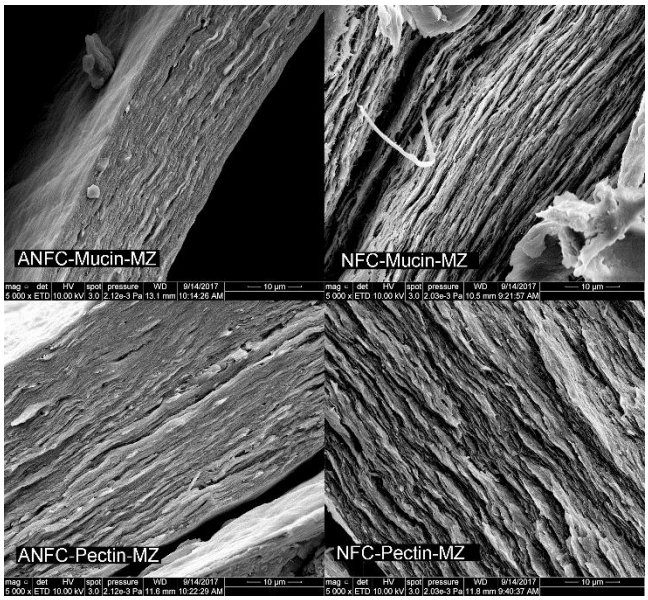

Fig. 6. SEM micrographs of ANFC and NFC films containing the mucoadhesive polymer and metronidazole at 5000 times magnification. Scale bar is 10 µm.

3.5 Drug release

Formulated films (1 cm^2) containing MZ and having selective mucoadhesive properties were used for the evaluation of drug release. The amount of MZ was set to 10% of the total weight of the film (i.e. total polymer content). MZ was fully dissolved in the hydrogel prior to the drying process. No loss of polymer or drug occurred during the film preparation due to the Teflon molds used, as the whole amount of hydrogel could be included in the final dry film. A tool with a set area of 1 cm^2 was used to cut the pieces for the drug release study, which enabled the calculation of the final drug content in the individual pieces. The drug release study was performed in order to study the effect of nanofibrillated cellullose grade (ANFC vs NFC) as well as the mucoadhesive polymer choice on the release profile of MZ. The cumulative release profiles are shown in Fig. 7. All formulations had a relatively high burst release of 20-40 % at the beginning up to 5 min depending on the formulation. This may indicate that MZ on the surface of the films was released relatively fast. After 15 min, the ANFC-Mucin-MZ and NFC-Mucin-MZ formulations had the highest drug release extent of 69.5 % and 65 % respectively. For NFC-Pectin-MZ and ANFC-Pectin-MZ the drug release after 15 min was lower with 60 % and 45 % of MZ release respectively. After 30 min the mucin containing formulations had overall a higher MZ release as opposed to the formulations with pectin. Among all formulations, the maximum drug release of 84.7 % at 30 min was observed for NFC–Mucin-MZ, while the minimum drug release of 59. 6 % at 30 min was obtained with ANFC–Pectin-MZ. Interestingly, these two polymer compositions had the highest mucoadhesiveness when measured without the model compound. The slight differences between ANFC and NFC could be explained with the apparent porosity observed in SEM images, where ANFC structure was denser than NFC, therefore resulting in slightly lower overall drug release from ANFC films when compared with NFC films.

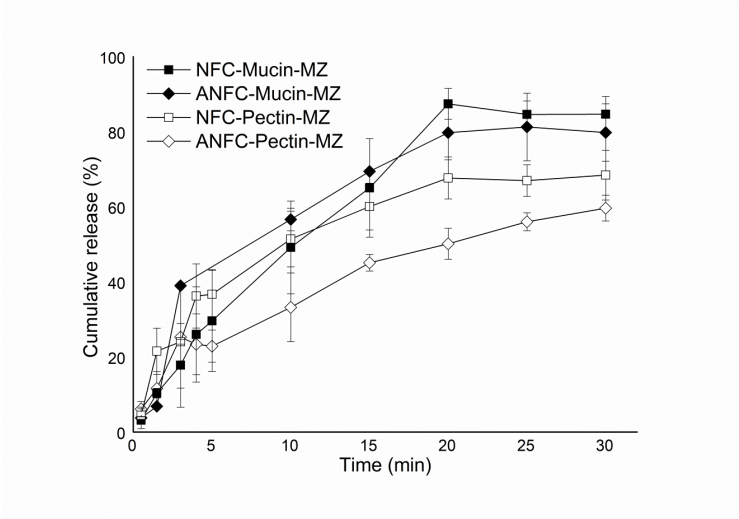

Fig. 7. Cumulative drug release profiles of MZ from mucoadhesive formulations (n = 3 ± stdev).

The pectin containing films had a higher thickness to begin with but also the thickness increased over 800% due to swelling and hydration during the 30 min drug release experiment (Table IV). The thickness of all films increased (398 - 873 %) during the 30 min period considerably more than the surface area (12 – 18 %) of the films. These values are slightly larger than the ones shown in Table III, indicating that the inclusion the hydrophilic MZ into the films did have an enhancing effect on the hydration of the films. The swelling of the lamellar films occurred mainly in the vertical direction. Therefore, the slower drug release seems reasonable from pectin containing formulations due to the swollen matrix and longer diffusion path. For buccal drug delivery applications all formulations exhibited rather suitable drug release profiles for MZ, as fast drug release would be advantageous from the batch into the mucosal membrane in oral cavity. Fast drug release combined with mucoadhesive properties (section 3.1) of the films would be beneficial for site specific drug delivery of MZ for e.g. treatment of periodontal diseases in the oral cavity.

Table IV. Dry thickness (from SEM images, n = 10), wet thickness (n = 5), thickness increase (n = 5) and area increase (n = 1) after 30 min exposure to the pH 6.8 phosphate buffer in drug release experiment conditions.

Formulation	Dry thickness (µm)	Wet thickness (µm)	Thickness increase (%)	Area increase (%)
ANFC	40.2 ± 1.0	344.8 ± 40.4	759 ± 91.0	18
ANFC-Mucin-MZ	97.6 ± 10.4	893.6 ± 22.1	816 ± 89.1	12
ANFC-Pectin-MZ	107.6 ± 6.9	1046.0 ± 84.2	873 ± 90.0	14
NFC	45.3 ± 1.5	326.0 ± 18.9	620 ± 41.5	16
NFC-Mucin-MZ	238.8 ± 5.3	1190.1 ± 44.7	398 ± 17.4	12
NFC-Pectin-MZ	228.2 ± 11.5	1453.5 ± 47.4	537 ± 32.3	13

3.6 Toxicity studies with TR146

Cytotoxicity studies were performed on human TR146 cell line cells, which have been shown previously as a useful tool to model human buccal epithelium (56,57). Mucoadhesive patches did not show any significant effect on TR146 viability after 24 h incubation (Fig. 8). MZ-containing patches however, were observed to lower cell viability slightly when compared with the control cells. This finding is supported by previous studies on MZ cytotoxicity, where 5 mM concentrations were found to affect the cell viability of Chinese hamster ovary, CHO, cells (58). The calculated amount of MZ ranged approximately 0.21 - 0.43 mg per film piece (Ø = 5 mm), which results in possible available concentration range of 6 - 12.7 mM of MZ per well depending on the film size after the drying process before cutting. Additionally, as shown in this study, MZ was rapidly released from the films (~ 30 min); therefore, the cytotoxicity was mostly due to MZ. The slightly lower viability values for pectin formulations might be explained with the heavier and thicker film size from which the pieces were cut, therefore causing slightly higher MZ concentrations in their respective wells.

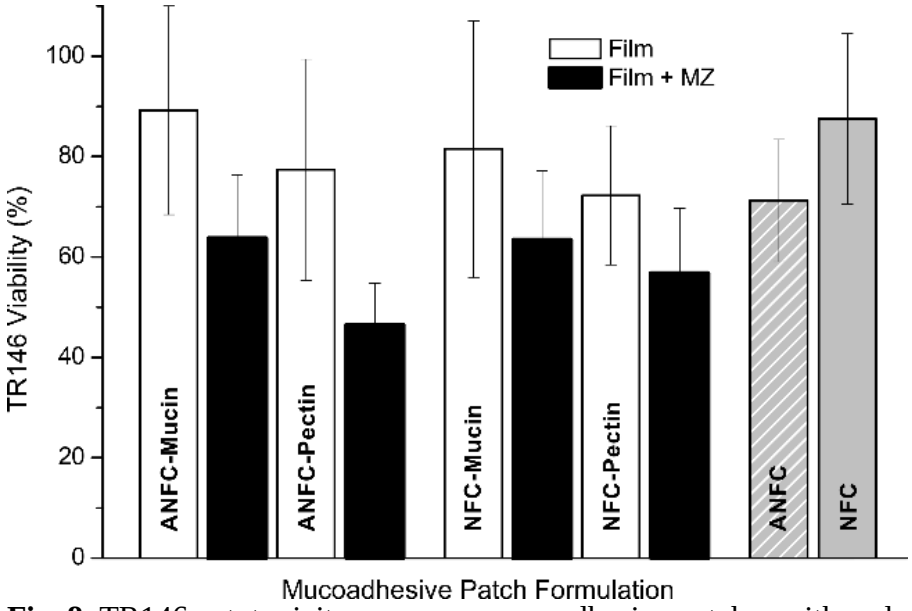

Fig. 8. TR146 cytotoxicity assays on mucoadhesive patches with and without MZ after 24 h incubation. Patches containing MZ showed slight cytotoxicity. Patches without the study compound did not have significant cytotoxic effects on the cells (n = 4 ± stdev).

4. Conclusions

All the bio-based polymers used in this study are regarded as non-toxic, biodegradable and from renewable sources. Every combination of NFC/ANFC and mucin/pectin/chitosan were found to enhance the mucoadhesive properties of the films. ANFC-Pectin and NFC-Mucin had the highest adhesion strength from the tested formulations. After administering the patch, the piece could be manually removed or swallowed, allowing the physiological cleansing mechanisms to dispose the

patch, eventually leaving no traces in the body. The texture analysis method used was very gentle in terms of applied force and contact time, which relates to actual use of the formulation. The drug release profile of metronidazole was fast for all films. This could be beneficial in treatment of oral diseases, such as periodontitis where high and rapid local dosing is desirable. The fast release rate ensures that the patch is inactive after detachment. TR146 cells were viable after 24 hours of incubation with film pieces. Slightly lower viability was observed in metronidazole containing pieces. Therefore, we suggest that natural cellulose based polymers NFC and ANFC could be used as an excellent film forming materials for mucoadhesive components such as mucin, pectin or chitosan as a functional mucoadhesive drug release application.

Acknowledgements

The financial support from Academy of Finland (Grant No. 258114) is gratefully acknowledged. Orion Foundation of the Professor Pool, Finland is greatly acknowledged.

5. References

1. Jones DS, Woolfson AD, Brown AF, Coulter WA, McClelland C, Irwin CR. Design, characterisation and preliminary clinical evaluation of a novel mucoadhesive topical formulation containing tetracycline for the treatment of periodontal disease. J Control Release. 2000;67:357-368.

2. Patel VF, Liu F, Brown MB. Modeling the oral cavity: In vitro and in vivo evaluations of buccal drug delivery systems. J Control Release 2012;161:746-756.

3. Deng Y, Yang F, Cocco E, Song E, Zhang J, Cui J, Mohideen M, Bellone S, Santin AD, Saltzman WM. Improved i.p. drug delivery with bioadhesive nanoparticles. Proc Natl Acad Sci U S A. 2016;113:11453-11458.

4. Pettit DK, Gombotz WR. The development of site-specific drug-delivery systems for protein and peptide biopharmaceuticals. Trends Biotechnol. 1998;16:343-349.

5. Giano MC, Ibrahim Z, Medina SH, Sarhane KA, Christensen JM, Yamada Y, Brandacher G, Schneider JP. Injectable bioadhesive hydrogels with innate antibacterial properties. Nat Commun. 2014;5:4095.

6. García MC, Aldana AA, Tártara LI, Alovero F, Strumia MC, Manzo RH, Martinelli M, Jimenez-Kairuz AF. Bioadhesive and biocompatible films as wound dressing materials based on a novel dendronized chitosan loaded with ciprofloxacin. Carbohydr Polym. 2017;175:75-86.

7. Fonseca-Santos B, Satake CY, Calixto GMF, dos Santos AM, Chorilli M. Trans-resveratrol-loaded nonionic lamellar liquid-crystalline systems: structural, rheological, mechanical, textural,

and bioadhesive characterization and evaluation of in vivo anti-inflammatory activity. Int J Nanomedicine. 2017;12:6883.

8. Jorfi M, Foster EJ. Recent advances in nanocellulose for biomedical applications. J Appl Polym Sci. 2015;132.

9. Halib N, Perrone F, Cemazar M, Dapas B, Farra R, Abrami M, Chiarappa G, Forte G, Zanconati F, Pozzato G, Murena L, Fiotti N, Lapasin R, Cansolino L, Grassi H, Grassi M. Potential Applications of Nanocellulose-Containing Materials in the Biomedical Field. Materials (Basel). 2017;10:977.

10. Märtson M, Viljanto J, Hurme T, Laippala P, Saukko P. Is cellulose sponge degradable or stable as implantation material? An in vivo subcutaneous study in the rat. Biomaterials. 1999;20:1989-1995.

11. Vartiainen J, Pöhler T, Sirola K, Pylkkänen L, Alenius H, Hokkinen J, Tapper U, Lahtinen P, Kapanen A, Putkisto K, Hiekkataipale P, Eronen P, Ruokolainen J, Laukkanen A. Health and environmental safety aspects of friction grinding and spray drying of microfibrillated cellulose. Cellulose. 2011;18:775-786.

12. Miron-Mendoza M, Seemann J, Grinnell F. The differential regulation of cell motile activity through matrix stiffness and porosity in three dimensional collagen matrices. Biomaterials. 2010;31:6425-6435.

13. Bhattacharya M, Malinen MM, Lauren P, Lou Y, Kuisma SW, Kanninen L, Lille M, Corlu A, GuGuen-Guillouzo C, Ikkala O, Laukkanen A, Urtti A, Yliperttula M. Nanofibrillar cellulose hydrogel promotes three-dimensional liver cell culture. J Control Release 2012;164:291-298.

14. Saito T, Kimura S, Nishiyama Y, Isogai A. Cellulose nanofibers prepared by TEMPO-mediated oxidation of native cellulose. Biomacromolecules. 2007;8:2485-2491.

15. Saito T, Nishiyama Y, Putaux J, Vignon M, Isogai A. Homogeneous suspensions of individualized microfibrils from TEMPO-catalyzed oxidation of native cellulose. Biomacromolecules. 2006;7:1687-1691.

16. Kolakovic R, Peltonen L, Laukkanen A, Hirvonen J, Laaksonen T. Nanofibrillar cellulose films for controlled drug delivery. Eur J Pharm Biopharm. 2012;82:308-315.

17. Kolakovic R, Peltonen L, Laukkanen A, Hellman M, Laaksonen P, Linder MB, Hirvonen J, Laaksonen T. Evaluation of drug interactions with nanofibrillar cellulose. Eur J Pharm Biopharm. 2013;85:1238-1244.

18. Lee K, Aitomäki Y, Berglund LA, Oksman K, Bismarck A. On the use of nanocellulose as reinforcement in polymer matrix composites. Composites Sci Technol. 2014;105:15-27.

19. Meneguin AB, Cury BSF, dos Santos AM, Franco DF, Barud HS, da Silva Filho EC. Resistant starch/pectin free-standing films reinforced with nanocellulose intended for colonic methotrexate release. Carbohydr Polym. 2017;157:1013-1023.

20. Laurén P, Somersalo P, Pitkänen I, Lou Y, Urtti A, Partanen J, Seppälä J, Madetoja M, Laaksonen T, Mäkitie A, Yliperttula M. Nanofibrillar cellulose-alginate hydrogel coated surgical sutures as cell-carrier systems. PLoS One. 2017;12:e0183487.

21. Lin N, Dufresne A. Nanocellulose in biomedicine: Current status and future prospect. Eur Polym J. 2014;59:302-325.

22. Salamat-Miller N, Chittchang M, Johnston TP. The use of mucoadhesive polymers in buccal drug delivery. Adv Drug Deliv Rev. 2005;57:1666-1691.

23. Svensson O, Arnebrant T. Mucin layers and multilayers—Physicochemical properties and applications. Curr Opin Colloid Interface Sci. 2010;15:395-405.

24. Linden S, Sutton P, Karlsson N, Korolik V, McGuckin M. Mucins in the mucosal barrier to infection. Mucosal Immunol. 2008;1:183-197.

25. Lieleg O, Ribbeck K. Biological hydrogels as selective diffusion barriers. Trends Cell Biol. 2011;21:543-551.

26. Bansil R, Turner BS. Mucin structure, aggregation, physiological functions and biomedical applications. Curr Opin Colloid Interface Sci. 2006;11:164-170.

27. Thirawong N, Nunthanid J, Puttipipatkhachorn S, Sriamornsak P. Mucoadhesive properties of various pectins on gastrointestinal mucosa: an in vitro evaluation using texture analyzer. Eur J Pharm Biopharm. 2007;67:132-140.

28. Zargar V, Asghari M, Dashti A. A review on chitin and chitosan polymers: structure, chemistry, solubility, derivatives, and applications. ChemBioEng Reviews. 2015;2:204-226.

29. Builders PF, Kunle OO, Okpaku LC, Builders MI, Attama AA, Adikwu MU. Preparation and evaluation of mucinated sodium alginate microparticles for oral delivery of insulin. Eur J Pharm Biopharm. 2008;70:777-783.

30. Ashton L, Pudney PDA, Blanch EW, Yakubov GE. Understanding glycoprotein behaviours using Raman and Raman optical activity spectroscopies: Characterising the entanglement induced conformational changes in oligosaccharide chains of mucin. Adv Colloid Interface Sci. 2013;199-200:66-77.

31. BeMiller JN. An introduction to pectins: structure and properties, in: An introduction to pectins: structure and properties. ACS Publications. 1986.

32. Huanbutta K, Cheewatanakornkool K, Terada K, Nunthanid J, Sriamornsak P. Impact of salt form and molecular weight of chitosan on swelling and drug release from chitosan matrix tablets. Carbohydr Polym. 2013;97:26-33.

33. El-Mahrouk GM, El-Gazayerly ON, Aboelwafa AA, Taha MS. Chitosan lactate wafer as a platform for the buccal delivery of tizanidine HCl: in vitro and in vivo performance. Int J Pharm. 2014;467:100-112.

34. Bruschi ML, Jones DS, Panzeri H, Gremião MP, De Freitas O, Lara EH. Semisolid systems containing propolis for the treatment of periodontal disease: in vitro release kinetics, syringeability, rheological, textural, and mucoadhesive properties. J Pharm Sci. 2007;96:2074-2089.

35. El-Kamel AH, Ashri LY, Alsarra IA. Micromatricial metronidazole benzoate film as a local mucoadhesive delivery system for treatment of periodontal diseases. AAPS PharmSciTech. 2007;8:E184-E194.

36. Zykwinska AW, Ralet MC, Garnier CD, Thibault JF. Evidence for in vitro binding of pectin side chains to cellulose. Plant Physiol. 2005;139:397-407.

37. Myllytie P, Salmi J, Laine J. The influence of pH on the adsorption and interaction of chitosan with cellulose. BioResources. 2009;4:1647-1662.

38. Cranston ED, Eita M, Johansson E, Netrval J, Salajková M Arwin H, Wågberg L. Determination of Young's modulus for nanofibrillated cellulose multilayer thin films using buckling mechanics. Biomacromolecules. 2011;12:961-969.

39. Henriksson M, Berglund LA, Isaksson P, Lindstrom T, Nishino T. Cellulose nanopaper structures of high toughness. Biomacromolecules. 2008;9:1579-1585.

40. Mohammadi P, Toivonen MS, Ikkala O, Wagermaier W, Linder MB. Aligning cellulose nanofibril dispersions for tougher fibers. Sci Rep. 2017;7:11860.

41. Fujisawa S, Okita Y, Fukuzumi H, Saito T, Isogai A. Preparation and characterization of TEMPO-oxidized cellulose nanofibril films with free carboxyl groups. Carbohydr Polym. 2011;84:579-583.

42. Lu J, Askeland P, Drzal LT. Surface modification of microfibrillated cellulose for epoxy composite applications. Polymer. 2008;49:1285-1296.

43. Orelma H, Filpponen I, Johansson L, Österberg M, Rojas OJ, Laine J. Surface functionalized nanofibrillar cellulose (NFC) film as a platform for immunoassays and diagnostics. Biointerphases. 2012;7:61.

44. Gum J. Mucin genes and the proteins they encode: structure, diversity, and regulation. Am J Respir Cell Mol Biol. 1992;7:557-557.

45. Sriamornsak P, Thirawong N, Weerapol Y, Nunthanid J, Sungthongjeen S. Swelling and erosion of pectin matrix tablets and their impact on drug release behavior. Eur J Pharm Biopharm. 2007;67:211-219.

46. Valo H, Arola S, Laaksonen P, Torkkeli M, Peltonen L, Linder MB, Serimaa R, Kuga S, Hirvonen J, Laaksonen T. Drug release from nanoparticles embedded in four different nanofibrillar cellulose aerogels. Eur J Pharm Sci. 2013;50:69-77.

47. Dick-Pérez M, Zhang Y, Hayes J, Salazar A, Zabotina OA, Hong M. Structure and interactions of plant cell-wall polysaccharides by two-and three-dimensional magic-angle-spinning solid-state NMR. Biochemistry (NY). 2011;50:989-1000.

48. Han C, Chen J, Wu X, Huang Y, Zhao Y. Detection of metronidazole and ronidazole from environmental Samples by surface enhanced Raman spectroscopy. Talanta. 2014;128:293-298.

49. Gnanasambandam R, Proctor A. Determination of pectin degree of esterification by diffuse reflectance Fourier transform infrared spectroscopy. Food Chem. 2000;68:327-332.

50. Sacui IA, Nieuwendaal RC, Burnett DJ, Stranick SJ, Jorfi M, Weder C, Foster EJ, Olsson RT, Gilman JW. Comparison of the properties of cellulose nanocrystals and cellulose nanofibrils isolated from bacteria, tunicate, and wood processed using acid, enzymatic, mechanical, and oxidative methods. ACS Appl Mater Interfaces. 2014;6:6127-6138.

51. De Gelder J, De Gussem K, Vandenabeele P, Moens L. Reference database of Raman spectra of biological molecules. J Raman Spectrosc. 2007;38:1133-1147.

52. Oh CM, Heng PWS, Chan LW. Influence of hydroxypropyl methylcellulose on metronidazole crystallinity in spray-congealed polyethylene glycol microparticles and its impact with various additives on Metronidazole release. AAPS PharmSciTech. 2015;16:1357-1367.

53. Zykwinska A, Thibault J, Ralet M. Competitive binding of pectin and xyloglucan with primary cell wall cellulose. Carbohydr Polym. 2008;74:957-961.

54. Cosgrove DJ. Re-constructing our models of cellulose and primary cell wall assembly. Curr Opin Plant Biol. 2014;22:122-131.

55. Gu J, Catchmark JM. The impact of cellulose structure on binding interactions with hemicellulose and pectin. Cellulose. 2013;20:1613-1627.

56. Jacobsen J, van Deurs B, Pedersen M, Rassing MR. TR146 cells grown on filters as a model for human buccal epithelium: I. Morphology, growth, barrier properties, and permeability. Int J Pharm. 1995;125:165-184.

57. Nielsen HM, Rassing MR. TR146 cells grown on filters as a model of human buccal epithelium: IV. Permeability of water, mannitol, testosterone and β-adrenoceptor antagonists. Comparison to human, monkey and porcine buccal mucosa. Int J Pharm. 2000;194:155-167.

58. Mahood J, Willson R. Cytotoxicity of metronidazole (Flagyl) and misonidazole (Ro-07-0582): enhancement by lactate. Br J Cancer. 1981;43:350-354.